Heatmap overlay using neutral body model for visualizing the measured gaze distributions of observers

Michiko Inoue, Fuyuko Iwasaki, Masashi Nishiyama, and Yoshio Iwai

Graduate School of Engineering, Tottori University, Japan
mi.inoue@tottori-u.ac.jp

Abstract. We propose a method for visualizing where an observer's gaze focuses on a subject in a still image using a neutral human body model. Generally, two-dimensional (2D) heatmaps are superimposed on still images to visualize an observer's gaze distribution, which indicates where an observer looks when observing a subject. To investigate gaze distributions, eye-tracking researchers need a method to directly compare the 2D heatmaps because body pose and shape differ among subjects. Thus, a comparison of the gaze distributions using the 2D heatmaps is time-consuming if there is no acceptable method to handle the body pose and shape variations. Instead, our visualization method superimposes a three-dimensional (3D) heatmap representing the gaze distribution on the surface of a neutral human body, which has a fixed pose and shape for all subjects to visualize the locations at which an observer's gaze focuses. Experimental results show that our visualization method allows eye-tracking researchers to compare gaze distributions more directly than the conventional visualization method using 2D heatmaps on still images.

Keywords: Gaze distribution · 3D heatmap · neutral body model · visualization · vertex attention probability.

1 Introduction

There are many situations in which people gather together, such as parties and conferences. Eye-tracking researchers in the computer vision and cognitive science fields investigate the gaze distributions of people in these situations, because these gaze distributions indicate the behavior of the observers when they look at the bodies of other people. For example, consider a situation in which some observers judge the aesthetics of subjects attending a ceremonial party. In this situation, the eye-tracking researchers measure the gaze distributions of the observers during this judgement. The researchers then compare the measured gaze distributions of the subjects to determine whether the gaze behaviors of the observers differ. To perform this comparison, it is necessary to visualize the gaze distribution so that the researchers can directly compare the locations on the subjects where the observers focus their attention.

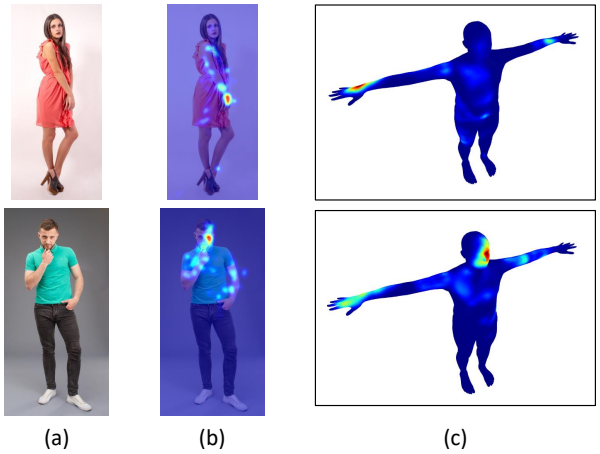

Fig. 1. (a) Measuring and visualizing where an observer's gaze focuses when they look at the subjects in the still images. (b) Superimposing the measured gaze distributions onto the images using 2D heatmaps. (c) Superimposing the distributions on a neutral human body model using 3D heatmaps.

We here consider how to compare whether there are differences in the measured gaze distributions of observers observing an attractive female and male subject. The body poses and shapes of the female and male subject are very different, as shown in the examples in Fig. 1(a). In these examples, the woman has both hands down, and the man has one hand up. Moreover, the woman is slender, and the man is muscular. As these examples illustrate, subjects have various body poses and various body shapes in such situations. Hence, eye-tracking researchers need a visualization method that can directly compare the gaze distributions among subjects, even when they have different body poses and body shapes.

Two-dimensional (2D) heatmaps are often superimposed on still images to visualize where an observer's gaze focuses on a subject. Figure 1(b) shows examples of this visualization. In fact, eye-tracking researchers have commonly used 2D heatmaps to represent gaze distributions [8, 6, 4]. However, body poses and shapes differ among subjects when this method is used. To compare where the gazes of observers focus in the examples in Fig. 1(b), eye-tracking researchers must pay attention to the different poses of the hands and arms and the different body shapes of the man and woman. Therefore, a visualization that superimposes 2D heatmaps on still images is time-consuming for eye-tracking researchers to analyze them. Other visualization methods [9, 10] have been proposed in which 3D heatmaps representing the gaze distributions are superimposed on the surface of artificial objects by aligning the shapes of known objects. It is easier for eye-tracking researchers to directly compare gaze focus on artificial objects with rigid body shapes in various poses. However, applying these methods [9, 10] to

human subjects is restricting because humans are non-rigid and have various body shapes in different poses.

Here, we propose a visualization method that superimposes 3D heatmaps on the surface of a neutral human body to directly compare the locations of observer gazes when the observers look at subjects in still images. We use a neutral human body model with a body pose and shape that are normalized among subjects. Our visualization method allows eye-tracking researchers to directly compare the gaze distributions on the common 3D surface of the neutral human body model, even if the body poses and shapes of the subjects in still images differ. Figure 1(c) shows examples of 3D heatmaps representing gaze distributions by superimposing them on the 3D surface of the neutral human body model. In our visualization, it is not necessary to consider the differences in the body poses and shapes of the subjects. In addition, the observer gaze distributions can be directly compared by simply looking at the spatially aligned 3D heatmaps superimposed on the surface of the neutral human body model.

2 Our 3D heatmap-based visualization method

2.1 Overview

In our method, the 3D heatmaps represent which parts of the subject's body the gazes of observers focus. The 3D heatmaps are superimposed on the surface of a neutral human body model. Figure 2 shows an overview of our method. Our method generates images visualizing the measured gaze distributions of the observer using steps S1 to S3 and the neutral human body model connecting these steps.

S1. Computation of the pixel attention probability
We calculate the probability that the gazes of observers focus on the 2D positions of the pixels in region of the subject in the still image. We call this the pixel attention probability.

S2. Computation of the vertex attention probability
Using the relationship between the 2D positions of the pixels of the subject region and the 3D positions of the surface of the neutral human model, we calculate the probability that the gazes focus on the vertices of the body model. We call this the vertex attention probability.

S3. 3D heatmap overlay
We superimpose the 3D heatmap representing the vertex attention probabilities onto the neutral human body model so that eye-tracking researchers can directly compare the gaze distributions among subjects. To do this, we generate an image visualizing each gaze distribution using the 3D heatmap.

Neutral human body model
We use a neutral human body model with a pre-determined constant body pose and shape parameters to fix the pose and shape of the subjects. The model consists of a set of 3D vertices and the adjacencies between them.

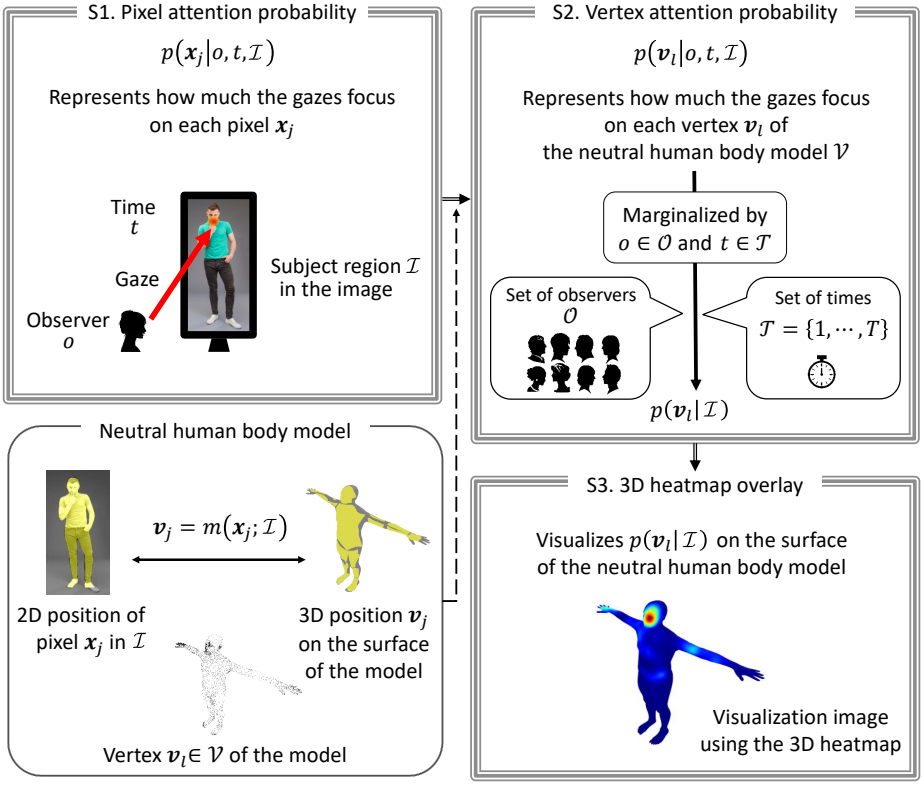

Fig. 2. Overview of our method. When observers look at a certain subject in a still image, we measure where their gazes focus on the subject, and visualize the gaze distribution using the 3D heatmap representing the vertex attention probability.

Our method transforms the 2D positions of the pixels in the subject region of the still image to the 3D positions on the surface of the neutral human body model.

Here, we discuss the issue of the conventional visualization method using the 2D heatmap representing the pixel attention probability. When body poses and shapes differ among subjects, the alignment of bodies in the subject regions causes gaps among the still images. Therefore, it is difficult to directly compare the pixel attention probability between subjects. Our method reduces the gap between body poses and shapes using neutral human body model with a normalized body pose in a normalized shape to represent the gaze distributions using the 3D heatmaps. Our visualization method enables the vertex attention probability among subjects with various body poses and shapes to be directly compared. In the following, we describe the pixel attention probability in Section 2.2, the neutral human body model in Section 2.3, the vertex attention

probability in Section 2.4, and the 3D heatmap for generating the visualization image in Section 2.5.

2.2 Pixel attention probability

Pixel attention probability indicates how much the measured gazes of the observers focus on each pixel in the subject region of the still image. Suppose that the subject region $\mathcal{I}$ is the set of pixels $\boldsymbol{x}_j$, and the gaze is measured from observer o at pixel $\boldsymbol{x}_t$ in the subject region $\mathcal{I}$ at time t. We denote the probability that the gaze is measured at a pixel $\boldsymbol{x}_j \in \mathcal{I}$ by

$$p(\boldsymbol{x}_j|o,t,\mathcal{I}) \sim \mathcal{N}(\boldsymbol{x}_j|\boldsymbol{x}_t,\boldsymbol{\Sigma}_p), \tag{1}$$

where $\mathcal{N}(\boldsymbol{x}_j|\boldsymbol{x}_t,\boldsymbol{\Sigma}_p)$ is a bivariate normal distribution with mean $\boldsymbol{x}_t$ and covariance matrix $\boldsymbol{\Sigma}_p$. We assume $\boldsymbol{\Sigma}_p = \mathrm{diag}\left(\sigma_p^2, \sigma_p^2\right)$. Here, $p(\boldsymbol{x}_j|o,t,\mathcal{I})$ is assumed to follow a normal distribution. The observer is not only looking at the pixel $\boldsymbol{x}_t$ where the gaze is measured and but also looking at the surrounding pixels. Hence, to approximate this, we use the normal distribution. Pixcel attention probability $p(\boldsymbol{x}_j|o,t,\mathcal{I})$ satisfies the following equation:

$$\sum_{\boldsymbol{x}_j \in \mathcal{I}} p(\boldsymbol{x}_j|o,t,\mathcal{I}) = 1. \tag{2}$$

Note that eye-tracking researchers must handle pixel attention probability carefully because it is difficult to directly compare pixel attention probabilities among subjects because body poses and shapes differ among subject regions in still images, as described in Section 1.

2.3 Neutral human body model

Several human body models [5, 2, 7] have been proposed to represent the human body with various poses and shapes. In these human body models, pose and shape are represented by continuous parameters in function space. We set up the neutral human body model using constant values for the parameters of body pose and shape for all subjects. This model allows us to transform different body poses and shapes into a common body representation for all subjects.

The neutral human body model $\mathcal{V}$ consists of meshes based on a set of vertices $\boldsymbol{v}_l$ and the adjacencies between vertices, as described in [5, 2, 7]. To indicate how much the gazes focus on a vertex $\boldsymbol{v}_l$, we could simply map pixel attention probability of each pixel $\boldsymbol{x}_j$ in the subject region of a still image to a vertex $\boldsymbol{v}_l$ of the neutral human body model using nearest neighbors. However, the $\boldsymbol{v}_l$ vertices are discrete, and this simple mapping will cause aliasing. For this reason, we use the 3D position $\boldsymbol{v}_j$ that exists continuously on the surface of the neutral human body model.

The method for mapping the 2D position of pixel $\boldsymbol{x}_j \in \mathcal{I}$ in the subject region of a still image to a 3D position $\boldsymbol{v}_j$ on the surface of a neutral human body model is as follows. Specifically, we transform it using function $m()$ as

$$\boldsymbol{v}_j = m(\boldsymbol{x}_j;\mathcal{I}). \tag{3}$$

The function $m()$ first estimates the body pose and shape parameters for each subject in the still image using an existing method, e.g. [3, 11, 1, 12]. Next, the estimated pose and shape parameters are converted to constant values for the neutral human body model. In this transformation, the 2D position of the pixel $\boldsymbol{x}_j$ can be automatically mapped to the 3D position $\boldsymbol{v}_j$.

2.4 Vertex attention probability

We define the vertex attention probability, which represents how much an observer o focuses his/her gaze on a vertex $\boldsymbol{v}_l$ of the neutral human body model $\mathcal{V}$ when looking at the subject region $\mathcal{I}$ at time t as

$$p(\boldsymbol{v}_l|o,t,\mathcal{I}) = \sum_{\boldsymbol{x}_j \in \mathcal{I}} p(\boldsymbol{v}_l|\boldsymbol{x}_j,\mathcal{I}) p(\boldsymbol{x}_j|o,t,\mathcal{I}), \tag{4}$$

where $p(\boldsymbol{v}_l|\boldsymbol{x}_j,\mathcal{I})$ is the probability that the gaze focuses on the 3D vertex $\boldsymbol{v}_l$ of the neutral human body model given the 2D pixel $\boldsymbol{x}_j \in \mathcal{I}$. We transform the 2D position of the pixel $\boldsymbol{x}_j$ on the still image to the 3D position $\boldsymbol{v}_j$ on the neutral human body model surface using Eq.(3) as

$$p(\boldsymbol{v}_l|o,t,\mathcal{I}) = \sum_{\boldsymbol{x}_j \in \mathcal{I}} p(\boldsymbol{v}_l|\boldsymbol{v}_j,\mathcal{I}) p(\boldsymbol{x}_j|o,t,\mathcal{I}). \tag{5}$$

Obtaining this probability using geodetic distances is computationally expensive. Therefore, we make the following assumption to reduce computation time. First, we suppose that the pixel at which the gaze focuses is transformed to 3D position $\boldsymbol{v}_j$ on the neutral human body model. A smaller Euclidean distance from $\boldsymbol{v}_j$ to vertex $\boldsymbol{v}_l$ on the neutral human body model means that the probability that the gaze is measured at that vertex will be higher. Based on this assumption, we express $p(\boldsymbol{v}_l|\boldsymbol{v}_j,\mathcal{I}) \simeq \mathcal{N}(\boldsymbol{v}_l|\boldsymbol{v}_j,\boldsymbol{\Sigma}_v)$ using a normal distribution and calculate the vertex attention probability $p(\boldsymbol{v}_l|o,t,\mathcal{I})$ as

$$p(\boldsymbol{v}_l|o,t,\mathcal{I}) \simeq \sum_{\boldsymbol{x}_j \in \mathcal{I}} \mathcal{N}(\boldsymbol{v}_l|\boldsymbol{v}_j,\boldsymbol{\Sigma}_v) p(\boldsymbol{x}_j|o,t,\mathcal{I}), \tag{6}$$

where $\mathcal{N}(\boldsymbol{v}_l|\boldsymbol{v}_j,\boldsymbol{\Sigma}_v)$ is a trivariate normal distribution with mean $\boldsymbol{v}_j$ and covariance matrix $\boldsymbol{\Sigma}_v$. In our method, the covariance matrix is $\boldsymbol{\Sigma}_v = \mathrm{diag}\left(\sigma_v^2, \sigma_v^2, \sigma_v^2\right)$. Note that $p(\boldsymbol{v}_l|o,t,\mathcal{I})$ satisfies the following equation:

$$\sum_{\boldsymbol{v}_l \in \mathcal{V}} p(\boldsymbol{v}_l|o,t,\mathcal{I}) = 1. \tag{7}$$

Here, we further enhance the comparison of gaze distributions in eye-tracking research. It is time-consuming to individually check the locations of gaze focus for each observer o and at each time t. We hence marginalize the probabilities using the set of observers $\mathcal{O}$ and set of measurement times $\mathcal{T}$. Given subject

region $\mathcal{I}$ in the still image, we calculate the marginal probability that the gazes are measured at the vertex $\boldsymbol{v}_l$ of the neutral human body model as follows:

$$p(\boldsymbol{v}_l|\mathcal{I}) = \sum_{o\in\mathcal{O},t\in\mathcal{T}} p(\boldsymbol{v}_l|o,t,\mathcal{I})p(o)p(t). \tag{8}$$

Let O be the number of elements in set $\mathcal{O}$ and T be the number of elements in set $\mathcal{T}$. Approximating $p(o)$ using the uniform distribution $1/O$ and $p(t)$ using the uniform distribution $1/T$, Eq.(8) is converted to

$$p(\boldsymbol{v}_l|\mathcal{I}) = \frac{1}{OT} \sum_{o\in\mathcal{O},t\in\mathcal{T}} p(\boldsymbol{v}_l|o,t,\mathcal{I}). \tag{9}$$

Note that $p(\boldsymbol{v}_l|\mathcal{I})$ satisfies the following equation:

$$\sum_{\boldsymbol{v}_l\in\mathcal{V}} p(\boldsymbol{v}_l|\mathcal{I}) = 1. \tag{10}$$

We call $p(\boldsymbol{v}_l|\mathcal{I})$ in Eq.(9) the vertex attention probability marginalized by the set of observers $\mathcal{O}$ and set of measurement times $\mathcal{T}$.

2.5 3D heatmap for generating the visualization image

To visualize the gaze distributions on a neutral body model for direct comparison among subjects, we represent the vertex attention probability $p(\boldsymbol{v}_l|\mathcal{I})$ using a 3D heatmap and overlay it onto the surface of the model. First, we consider a simple, vertex-only heatmap visualization. Figure 3(a) shows examples of the visualization images using the vertex-only heatmap. In the figure, vertices with a higher probability of concentrated gazes are redder in hue, and those with a lower probability of focused gazes are closer to blue. In these visualization images, the front and back vertices of the neutral human body model are both visible, making it difficult to compare the gaze distributions among subjects. Thus, we continuously interpolate the colors representing the high and low probabilities of focused gazes at 3D positions $\boldsymbol{v}_j$ using a mesh on the surface of the neutral human body model. Figure 3(b) shows examples of the visualization images using the 3D mesh heatmap. This heatmap representation prevents the front and back of the neutral human body model from being visible simultaneously, making it easier to directly to compare the gaze distributions among subjects.

3 Experiments

3.1 Visualization images generation conditions

We evaluated the effectiveness of our method using visualization images generated by the following methods.

– Conventional method (M_{2d}): We overlaid the 2D heatmap representing the pixel attention probability described in Section 2.2 onto the still image.

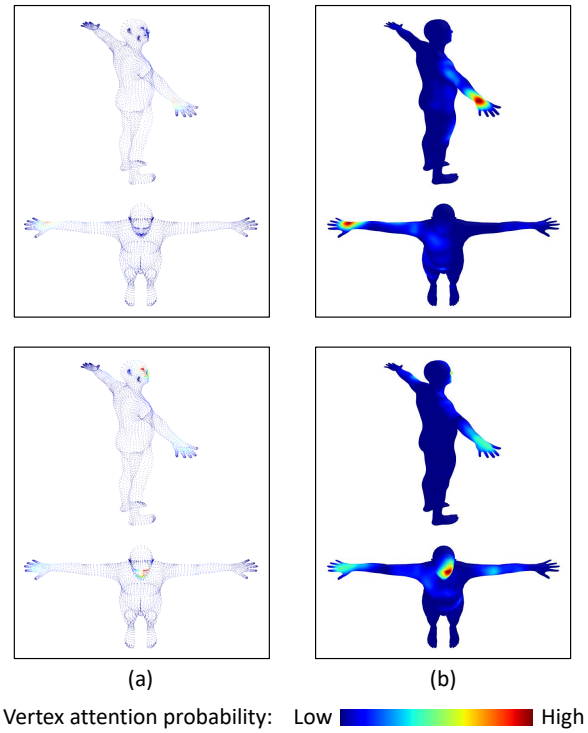

Fig. 3. Examples of visualization images using 3D heatmaps to represent vertex attention probabilities. (a) Using vertices only. (b) Using a 3D mesh.

– Our method (M_{3d}): We overlaid the 3D heatmap representing the vertex attention probability described in Section 2.4 onto the surface of the neutral human body model.

Note that the conventional method M_{2d} is equivalent to a visualization of the measured gaze distributions of observers, such as the methods used in existing analytical studies [8, 6, 4].

For our method M_{3d}, we used SMPL [5] to implement the neutral human body model described in Section 2.3. In the neutral human model used in this experiment, we set the pose and shape parameters of SMPL to their default values[1]. These default values specify that the body pose is one with arms outstretched and legs slightly open, and the body shape is average. The number of SMPL vertices used was 6890. Adjacency was represented by the meshes of triangles connecting the three vertices. We used DensePose [3] to estimate the body pose and shape parameters of SMPL for each subject in the still image for function $m()$ of Eq.(3), as described in Section 2.3.

[1] https://smpl.is.tue.mpg.de

3.2 Gaze measurement

To obtain measured gaze distributions, we asked several observers the following question Q so that they would evaluate the aesthetics of a subject in still images.

Q**:** Do you think that the subject's hands are beautiful?

We instructed them to answer "yes" or "no." The number of observers was 24 (12 men and 12 women), and the mean age of the observers was 22.4 ± 1.0 years old.

We first explained question Q to the observers and showed them a randomly selected still image on a display for 7 s. Figure 4(a) shows the still image given to the observers as a stimulus. Subject 1 is a slender woman with her right hand down and left leg slightly shifted forward. Subject 2 is a man with his right hand raised and his legs shoulder-width apart. Subject 3 is a petite woman with her right hand on her hip and her heels together. Figure 4(b) shows the subject regions in the still images.

We measured each observer's gaze using an eye tracker device while displaying the still image. This gaze measurement was repeated until all still images were viewed. The observers were seated 65 cm from the display. We allowed the observers to adjust the chair height so that the eye height was between 110 and 120 cm. We used a 24-inch display with a resolution of 1920×1080 pixels and a Gazepoint GP3 HD eye tracker with a 60 Hz sampling rate. The spatial resolution error of the eye tracker device is approximately one degree, as described in the specifications. We displayed the still image at a random position on the display to avoid center bias.

3.3 Visualization results

Figure 4(c) shows the visualization images generated using the conventional method M_{2d}, which superimposes the 2D heatmaps representing the pixel attention probability on the still images. Because of the variation in the body alignment among subjects, we must consider the differences in the body poses and shapes when comparing the gaze distributions. With these differences in mind, we can infer the following when comparing the results of Fig. 4(c). For subject 1, the observers' gazes focused most often on the right hand, followed by the head. For subject 2, the observers' gazes focused most often on the right hand, followed by the head and left hand. For subject 3, the observers' gazes focused most often on the right and left hands, followed by the head. From these results, we conclude that when question Q is given to observers looking at subjects 1 through 3, the gazes mostly focus on the hands and then on the head.

Figure 4(d) shows the visualization images generated using our method M_{3d}. Our visualization results show that the body poses and shapes of the neutral human body model are the same for all subjects. These 3D heatmaps make the body alignment equal for all subjects so that when analyzing differences in the gaze distributions, eye-tracking researchers only need to compare the same positions on the surface of the model. The gaze distributions for subjects 1

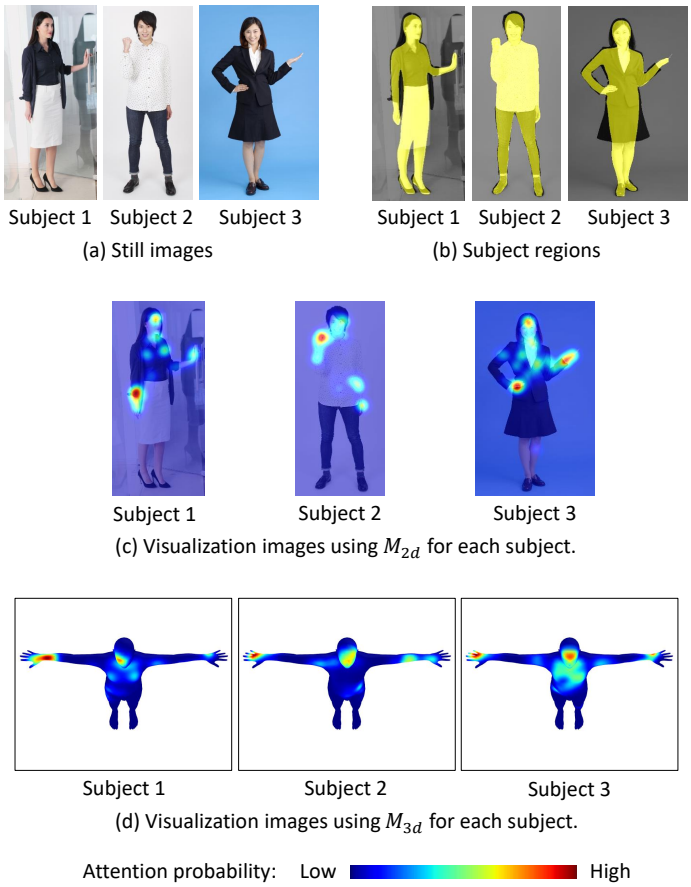

Fig. 4. Visualization image results showing the attention probabilities of the measured gaze distributions of observers looking at the still images.

through 3 reveal that the gazes most often focus on the hand, followed by the head. We can reach this conclusion more directly using our method M_{3d} than when using the conventional method M_{2d}.

3.4 Subjective assessment of the visualization images

Conditions of subjective assessment

We conducted a subjective assessment to determine whether the visualization images generated by the conventional method M_{2d} or those generated by our method M_{3d} enable the gaze distributions for various subjects to be directly compared. Sixteen eye-tracking researchers participated in the subjective assessment (13 men and three women). These researchers are graduate students studying human and computer vision, including gaze measurement

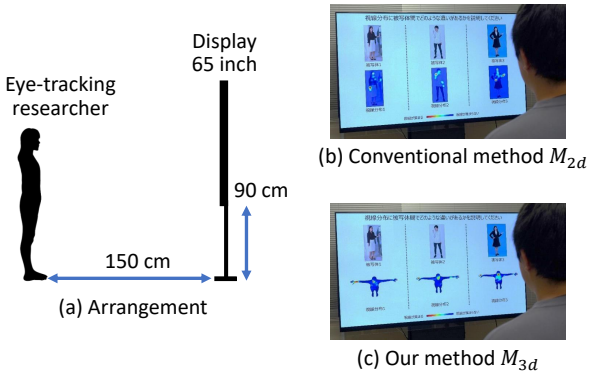

Fig. 5. Setup of the subjective assessment.

and analysis. Their average age was 23.4 ± 1.5 years old. Figure 5(a) shows the setup of the subjective assessment. The researchers stood upright at a distance of 150 cm horizontally from the display. The size of the display (LG, OLED65E9PJA) was 65 inches, and the height from the floor to the display was 90 cm. The researchers compared the results obtained using the conventional method M_{2d} (Figure 5(b)) with the results obtained using our method M_{3d} (Figure 5(c)). Visualization images of each method were shown on the display for 60 s each. We randomized the order of displaying the visualization images generated by M_{2d} and M_{3d}. We asked the researchers to choose the visualization images they felt would better directly facilitate the comparison of gaze distributions among the subjects. The researchers replied with one of the following answers: M_{2d}, M_{3d}, or neutral.

Result of the subjective assessment

Figure 6 shows the result of the subjective assessment. Five eye-tracking researchers chose the conventional method, two chose neutral, and nine chose our method. Our method M_{3d} obtained the highest results. Some researchers chose the conventional method M_{2d} because they were familiar with the 2D heatmaps on still images, which made it easy to identify the body parts focused on by gaze for each subject. In contrast, some researchers chose our method M_{3d} because the body parts such as the hands, torso, and legs are completely aligned for all subjects, so it is easy to compare the differences in the gaze distributions without having to pay attention to the body poses and shapes. From these results, we confirmed that our method M_{3d} enables eye-tracking researchers to more directly compare differences in the gaze distributions, even when the body poses and shapes are different, than the conventional method M_{2d}.

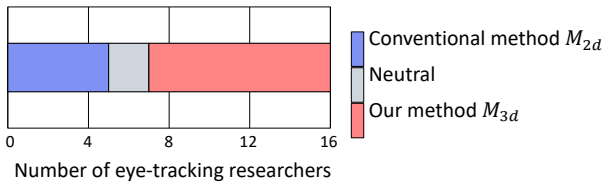

Fig. 6. Result of the subjective assessment comparing visualization images generated using the proposed and conventional methods.

4 Conclusions

We proposed a method of superimposing 3D heatmaps on the surface of a neutral human body model to visualize where the gazes of observers focus when they look at subjects in still images. For the visualization images obtained using our method, we confirmed in a subjective assessment that eye-tracking researchers could directly compare the gaze distributions, even when the body poses and shapes differed among subjects.

In future work, we will expand the evaluation to consider the case in which various shape characteristics, such as the weight, of the subjects in still images change. We also plan to consider the error estimation due to the influence of gender and clothing according to the neutral human body model. Furthermore, we intend to develop a method for calculating the vertex attention probability when there are multiple subjects in a single still image.

Acknowledgment

This work was partially supported by JSPS KAKENHI Grant No. JP23K11145. We would like to thank Mr. Ken Kinoshita for his cooperation in our evaluation and data collection.

References

1. Choutas, V., Müller, L., Huang, C.P., Tang, S., Tzionas, D., Black, M.J.: Accurate 3d body shape regression using metric and semantic attributes. In: Proceedings of the IEEE/CVF Conference on Computer Vision and Pattern Recognition. pp. 2718–2728 (2022)
2. Georgios, P., Choutas, V., Ghorbani, N., Bolkart, T., Osman, A.A.A., D.Tzionas, Black, M.J.: Expressive body capture: 3D hands, face, and body from a single image. In: Proceedings of the IEEE/CVF Conference on Computer Vision and Pattern Recognition. pp. 10975–10985 (2019)
3. Güler, R., Neverova, N., Kokkinos, I.: Densepose: Dense human pose estimation in the wild. In: Proceedings of the IEEE/CVF Conference on Computer Vision and Pattern Recognition. pp. 7297–7306 (2018)

4. Irvine, K.R., McCarty, K., Pollet, T.V., Cornelissen, K.K., Tovée, M.J., Cornelissen, P.L.: The visual cues that drive the self-assessment of body size: Dissociation between fixation patterns and the key areas of the body for accurate judgement. Body Image **29**, 31–46 (2019)
5. Matthew, M., Mahmood, N., Romero, J., Pons-Moll, G., Black, M.: SMPL: A skinned multi-person linear model. ACM Transactions on Graphics **34**(6), 1–16 (2015)
6. Nummenmaa, L., Jari, H., Santtila, P., Hyönä, J.: Gender and visibility of sexual cues influence eye movements while viewing faces and bodies. Archives of Sexual Behavior **41**(6), 1439–1451 (2012)
7. Osman, A.A.A., Bolkart, T., Tzionas, D., Black, M.J.: SUPR: A sparse unified part-based human representation. In: Proceedings of European Conference on Computer Vision. pp. 1–18 (2022)
8. Piers, C., Peter, H., Kiviniemi, V., Hannah, G., Martin, T.: Patterns of eye movements when male and female observers judge female attractiveness, body fat and waist-to-hip ratio. Evolution and Human Behavior **30**(6), 417–428 (2009)
9. Takahashi, R., Suzuki, H., Chew, J., Ohtake, Y., Nagai, Y., Ohtomi, K.: A system for three-dimensional gaze fixation analysis using eye tracking glasses. Journal of Computational Design and Engineering **5**(4), 449–457 (2017)
10. Wang, X., Lindlbauer, D., Lessig, C., Maertens, M., Alexa, M.: Measuring the visual salience of 3d printed objects. IEEE Computer Graphics and Applications **36**(4), 46–55 (2016)
11. Xiu, Y., Yang, J., Tzionas, D., Black, M.J.: Icon: Implicit clothed humans obtained from normals. In: Proceedings of the IEEE/CVF Conference on Computer Vision and Pattern Recognition. pp. 13296–13306 (2022)
12. Zhang, H., Tian, Y., Zhou, X., Ouyang, W., Liu, Y., Wang, L., Sun, Z.: Pymaf: 3d human pose and shape regression with pyramidal mesh alignment feedback loop. In: Proceedings of the IEEE/CVF International Conference on Computer Vision. pp. 11446–11456 (2021)